

# Quasi-LPV Modelling and Non-Linear Identification of a Twin Rotor System

Fatiha Nejjari, Damiano Rotondo, Vicenç Puig and Mario Innocenti

**Abstract**—This paper describes the experimental identification of the parameters of the Twin Rotor MIMO System (TRMS) non-linear model using data collected from the real lab set-up. From this non-linear model, a quasi-linear parameter varying (quasi-LPV) model has also been derived using a state transformation. This quasi-LPV model is approximated with a polytopic model using the bounding box approach. Such a model can later be used for control design. The model parameters have been calibrated by means of non-linear least-squares identification approach. Once the calibrated non-linear model has been obtained, a simulator has been built and validated against real data showing satisfactory results when compared to real data.

## I. INTRODUCTION

The TRMS is an aero-dynamical system similar to a helicopter (see Fig. 1). At both ends of its beam there are two propellers driven by DC motors, each perpendicular to the other one. The beam can rotate freely in the horizontal and vertical planes, in such a way that its ends move on spherical surfaces. The joined beam can be moved by changing the motors supply voltages, thus controlling the rotational speed of the propellers. There is a counter-weight fixed to the beam which is used for balancing the angular momentum in a stable equilibrium position. The rotor generating the vertical movement is called the main rotor. It enables the TRMS to pitch, which is a rotation in the vertical plane around the horizontal axis. The rotor generating the horizontal movement is called the tail rotor. It enables the model to yaw, which is a rotation in the horizontal plane around the vertical axis. The system is perceived as a challenging control engineering problem owing to its high non-linearity, cross-coupling between its two axes, frictions, saturations and inaccessibility of some of its states and outputs for measurements. Because of all these features, obtaining a non-linear model calibrated from data collected from the real set-up is a hard task.

The modelling of such a system has been addressed in several papers. In particular, in [1] two physical models based on Newtonian and Lagrangian approaches are presented and compared. Further modelling improvements can be found in [2], [3] and [4]. Looking at those models the reader can

This work has been funded by the Spanish MINECO through the project CYCYT SHERECS (ref. DPI2011-26243), by the European Commission through contract i-Sense (ref. FP7-ICT-2009-6-270428) and by UPC through the grant FPI-UPC E-01104.

Fatiha Nejjari, Damiano Rotondo and Vicenç Puig are with Advanced Control Systems Group (SAC), Universitat Politècnica de Catalunya (UPC), Rambla de Sant Nebridi, 11, 08222 Terrassa, Spain (e-mail: vicenc.puig@upc.edu). Mario Innocenti is with Dipartimento di Sistemi Elettrici e Automazione, Facoltà di Ingegneria, Università di Pisa, Italy (e-mail: minnoce@dsea.unipi.it).

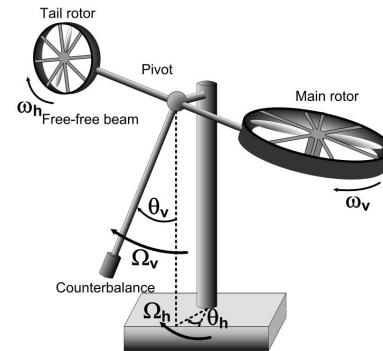


Fig. 1. Components of the Twin Rotor MIMO System

realize about the high non-linearity and cross-coupling of such a system. Regarding the experimental identification of the parameters of the TRMS model some preliminary work can be found in [5], [6], [7], [8] and [9].

In this work, the non-linear model of the TRMS system proposed in [4] is identified using real data taken from the lab set-up. Moreover, from this non-linear model, a quasi-LPV model is derived using the approach proposed by [10]. The quasi-LPV model is then approximated in a polytopic fashion using the *bounding box* approach. The polytopic quasi-LPV model can later be used for designing controllers for the TRMS system.

At first, standard linear identification techniques [11] were applied to estimate the parameters of the TRMS non-linear model. Good models have been obtained around some given operating point, but the overall model failed in reproducing the system behavior in operating points different from the ones used during the identification. This is mainly due to the high non-linearity of the model. For this reason, a non-linear system identification approach has finally been used. This paper presents the results obtained solving several non-linear least square problems.

Once the calibrated non-linear model has been obtained, a simulator has been built and validated showing satisfactory results when compared to real data.

The structure of the paper is the following: In Section II, a quasi-LPV model is derived from the non-linear model of the TRMS system proposed in [4]. The non-linear identification approach used to estimate the parameters of the model is described in Section III and the results are presented in Section IV. Section V presents the validation of the calibrated model using real data. Finally, the main conclusions are summarized in Section VI.

## II. TWIN ROTOR MIMO SYSTEM MODELLING

### A. Non-linear modelling

The strategy to model the TRMS is to split the system into simpler subsystems: the DC-Motors, the propellers and the beam. The first two have independent dynamics, that is, the main motor does not affect the behaviour of the tail motor, and vice versa. The same is true for the propellers. On the other hand, the dynamics of the beam is strongly non-linear with the presence of interaction phenomena among the horizontal and the vertical dynamics. Using such a modelling approach, the following non-linear model has been proposed in [4] introducing some improvement to the existing models already proposed in the literature ([1], [2], [3]):

$$\frac{d\omega_h}{dt} = \frac{k_a k_1}{J_{tr} R_a} u_h - \left( \frac{B_{tr}}{J_{tr}} + \frac{k_a^2}{J_{tr} R_a} \right) \omega_h - \frac{f_1(\omega_h)}{J_{tr}} \quad (1)$$

$$\frac{d\Omega_h}{dt} = \frac{l_t f_2(\omega_h) \cos \theta_v - k_{oh} \Omega_h - f_3(\theta_h) + f_6(\theta_v)}{D \cos^2 \theta_v + E \sin^2 \theta_v + F} + \frac{k_m \omega_v \sin \theta_v \Omega_v (D \cos^2 \theta_v - E \sin^2 \theta_v - F - 2E \cos^2 \theta_v)}{(D \cos^2 \theta_v + E \sin^2 \theta_v + F)^2} + \frac{k_m \cos \theta_v \left( \frac{k_a k_2}{R_a} u_v - \left( B_{mr} + \frac{k_a^2}{R_a} \right) \omega_v - f_4(\omega_v) \right)}{J_{mr} (D \cos^2 \theta_v + E \sin^2 \theta_v + F)} \quad (2)$$

$$\frac{d\theta_h}{dt} = \Omega_h \quad (3)$$

$$\frac{d\omega_v}{dt} = \frac{k_a k_2}{J_{mr} R_a} u_v - \left( \frac{B_{mr}}{J_{mr}} + \frac{k_a^2}{J_{mr} R_a} \right) \omega_v - \frac{f_4(\omega_v)}{J_{mr}} \quad (4)$$

$$\frac{d\Omega_v}{dt} = \frac{l_m f_5(\omega_v) + k_g \Omega_h f_5(\omega_v) \cos \theta_v - k_{ov} \Omega_v}{J_v} + \frac{g((A-B) \cos \theta_v - C \sin \theta_v) - \Omega_h^2 H \sin \theta_v \cos \theta_v}{J_v} + \frac{k_t \left( \frac{k_a k_1}{R_a} u_h - \left( B_{tr} + \frac{k_a^2}{R_a} \right) \omega_h - f_1(\omega_h) \right)}{J_v J_{tr}} \quad (5)$$

$$\frac{d\theta_v}{dt} = \Omega_v \quad (6)$$

The non-linear functions  $f_i$ , that take into account the frictions and coupling effects between horizontal/vertical dynamics, are defined as follows:

$$f_1(\omega_h) = \begin{cases} k_{thp} \omega_h^2 & \text{if } \omega_h \geq 0 \\ -k_{thm} \omega_h^2 & \text{if } \omega_h < 0 \end{cases} \quad (7)$$

$$f_2(\omega_h) = \begin{cases} k_{fhp} \omega_h^2 & \text{if } \omega_h \geq 0 \\ -k_{fhm} \omega_h^2 & \text{if } \omega_h < 0 \end{cases} \quad (8)$$

$$f_3(\theta_h) = \begin{cases} k_{chp} \theta_h & \text{if } \theta_h \geq 0 \\ -k_{chm} \theta_h & \text{if } \theta_h < 0 \end{cases} \quad (9)$$

$$f_4(\omega_v) = \begin{cases} k_{thp} \omega_v^2 & \text{if } \omega_v \geq 0 \\ -k_{thm} \omega_v^2 & \text{if } \omega_v < 0 \end{cases} \quad (10)$$

$$f_5(\omega_v) = \begin{cases} k_{fvp} \omega_v^2 & \text{if } \omega_v \geq 0 \\ -k_{fvn} \omega_v^2 & \text{if } \omega_v < 0 \end{cases} \quad (11)$$

$$f_6(\theta_v) = \begin{cases} k_{cvp} (\theta_v - \theta_v^0)^2 & \text{if } \theta_v \geq \theta_v^0 \\ -k_{cvn} (\theta_v - \theta_v^0)^2 & \text{if } \theta_v < \theta_v^0 \end{cases} \quad (12)$$

The system input vector is  $u = [u_h, u_v]^T$  where  $u_h$  is the input voltage of the tail motor and  $u_v$  is the input voltage

of the main motor. On the other hand, the system states are  $x = [\omega_h, \Omega_h, \theta_h, \omega_v, \Omega_v, \theta_v]^T$  where  $\Omega_h$  is the angular velocity around the vertical axis,  $\theta_h$  is the yaw angle of the beam (horizontal plane),  $\omega_h$  is the rotational velocity of the tail rotor,  $\Omega_v$  is the angular velocity around the horizontal axis,  $\theta_v$  is the pitch angle of the beam (vertical plane) and  $\omega_v$  is the rotational velocity of the main rotor.  $J_{tr/mr}$  are the moments of inertia in DC-motor tail/main propeller subsystem, respectively.  $\theta_v^0$  is the equilibrium value for the vertical angle when no input voltage acts on the main propeller. The constants of the non-linear model (1)-(6) are defined as:

$$\begin{aligned} A &= (m_t/2 + m_{tr} + m_{ts}) l_t & B &= (m_m/2 + m_{mr} + m_{ms}) l_m \\ C &= m_{cb} l_{cb} + m_b l_b / 2 & H &= A l_t + B l_m + m_b l_b^2 / 2 + m_{cb} l_{cb}^2 \\ D &= m_b l_b^2 / 3 + m_{cb} l_{cb}^2 & F &= m_{ms} r_{ms}^2 + m_{ts} r_{ts}^2 / 2 \\ E &= (m_{mr} + m_{ms} + m_m / 3) l_m^2 + (m_{tr} + m_{ts} + m_t / 3) l_t^2 \end{aligned}$$

where  $m_{ms}$  and  $m_{ts}$  are the masses of the main and tail shields,  $m_m$  and  $m_t$  are the masses of the main and the tail parts of the beam,  $m_{mr}$  and  $m_{tr}$  are the masses of the main and the tail DC-motor with main and tail rotor,  $m_b$  and  $l_b$  are the mass and the length of the counter-weight beam,  $m_{cb}$  and  $l_{cb}$  represent the mass of the counter-weight and the distance between the counter-weight and the joint and  $r_{ms}$  and  $r_{ts}$  are the radius of the main and tail shield.

### B. Quasi-LPV modelling of TRMS

To take into account the TRMS high non-linearity and cross-coupling between its two axes, an accurate dynamic model of the system is thus required to achieve control objectives satisfactorily. A quasi-LPV system is defined as a linear time-varying plant whose state-space matrices are fixed functions of some vector of varying parameters  $\psi_t$  that depend on the state variables. Then, it is described by state-space equations of the form:

$$\dot{x}(t) = A(\psi_t) x(t) + B(\psi_t) u(t) \quad (13)$$

where  $x(t) \in R^{n_x}$  represents the state vector and  $u(t) \in R^{n_u}$  denotes the control inputs. Here  $A(\psi_t) \in R^{n_x \times n_x}$  and  $B(\psi_t) \in R^{n_x \times n_u}$  are parameter-varying matrices.

Following the non-linear embedding in the parameters approach proposed in [10], the non-linear model (1)-(6) can be expressed in quasi-LPV form by:

$$\begin{bmatrix} \dot{\omega}_h(t) \\ \dot{\Omega}_h(t) \\ \dot{\theta}_h(t) \\ \dot{\omega}_v(t) \\ \dot{\Omega}_v(t) \\ \dot{\theta}_v(t) \end{bmatrix} = A(\psi_t) \begin{bmatrix} \omega_h(t) \\ \Omega_h(t) \\ \theta_h(t) \\ \omega_v(t) \\ \Omega_v(t) \\ \theta_v(t) - \theta_v^0 \end{bmatrix} + B(\psi_t) \begin{bmatrix} u_h(t) \\ u_v(t) \end{bmatrix} \quad (14)$$

$$A(\psi_t) = \begin{bmatrix} \psi_t^1(p_t) & 0 & 0 & 0 & 0 & 0 \\ \psi_t^2(p_t) & \psi_t^3(p_t) & \psi_t^4(p_t) & \psi_t^5(p_t) & \psi_t^6(p_t) & \psi_t^7(p_t) \\ 0 & 1 & 0 & 0 & 0 & 0 \\ 0 & 0 & 0 & \psi_t^8(p_t) & 0 & 0 \\ \psi_t^9(p_t) & \psi_t^{10}(p_t) & 0 & \psi_t^{11}(p_t) & a_{55} & \psi_t^{12}(p_t) \\ 0 & 0 & 0 & 0 & 1 & 0 \end{bmatrix} \quad (15)$$

$$B(\Psi_t) = \begin{bmatrix} b_{11} & 0 & 0 & 0 & b_{51} & 0 \\ 0 & \Psi_t^{13}(p_t) & 0 & b_{42} & 0 & 0 \end{bmatrix}^T$$

with:

$$\begin{aligned} \Psi_t^1(p_t) &= -\frac{k_a^2/R_a + B_{tr} + f_1(\omega_h)/\omega_h}{J_{tr}}, & \Psi_t^2(p_t) &= \frac{l_t \cos \theta_v f_2(\omega_h)/\omega_h}{D \cos^2 \theta_v + E \sin^2 \theta_v + F} \\ \Psi_t^3(p_t) &= -\frac{k_{oh}}{D \cos^2 \theta_v + E \sin^2 \theta_v + F}, & \Psi_t^4(p_t) &= -\frac{f_3(\theta_h)/\theta_h}{D \cos^2 \theta_v + E \sin^2 \theta_v + F} \\ \Psi_t^5(p_t) &= -\frac{k_m \left( \frac{k_a^2}{R_a} + B_{mr} + f_4(\omega_v)/\omega_v \right) \cos \theta_v}{(D \cos^2 \theta_v + E \sin^2 \theta_v + F) J_{mr}} \\ \Psi_t^6(p_t) &= \frac{k_m \omega_v \sin \theta_v (D \cos^2 \theta_v - E \sin^2 \theta_v - F - 2E \cos^2 \theta_v)}{(D \cos^2 \theta_v + E \sin^2 \theta_v + F)^2} \\ \Psi_t^7(p_t) &= \frac{f_6(\theta_v)/(\theta_v - \theta_v^0)}{D \cos^2 \theta_v + E \sin^2 \theta_v + F} \\ \Psi_t^8(p_t) &= -\frac{\frac{k_a^2}{R_a} + B_{mr} + f_4(\omega_v)}{J_{mr}}, & \Psi_t^9(p_t) &= \frac{-k_t (B_{tr} + f_1(\omega_h)/\omega_h + k_a^2/R_a)}{J_v J_{tr}} \\ \Psi_t^{10}(p_t) &= \frac{k_g \cos \theta_v f_5(\omega_v)/\omega_v - \Omega_h H \sin \theta_v \cos \theta_v}{J_v}, & \Psi_t^{11}(p_t) &= \frac{l_m f_5(\omega_v)/\omega_v}{J_v} \\ a_{55} &= -\frac{k_{ov}}{J_v}, & \Psi_t^{12}(p_t) &= \frac{g((A-B) \cos \theta_v - C \sin \theta_v)}{J_v (\theta_v - \theta_v^0)}, & b_{11} &= \frac{k_a k_1}{J_{tr} R_a} \\ \Psi_t^{13}(p_t) &= \frac{k_m \cos(\theta_v) k_a k_2}{(D \cos^2 \theta_v + E \sin^2 \theta_v + F) R_a J_{mr}}, & b_{42} &= \frac{k_a k_2}{J_{mr} R_a}, & b_{51} &= \frac{k_a k_1 k_t}{J_v J_{tr} R_a} \end{aligned}$$

$\Psi_t$  is the vector of varying parameters scheduled by  $p_t = [\theta_h \ \theta_v \ \omega_h \ \omega_v \ \Omega_h]^T$ . Notice that the vector  $p_t$  does not contain the state  $\Omega_v$  as this state variable does not affect the values of the elements in the model (14).

### C. Polytopic Quasi-LPV Representation

In [12] and [13], linear matrix inequality techniques are applied for gain-scheduled control of LPV systems. These techniques have been developed for LPV systems whose time-varying parameter vector  $\Psi_t$  varies within a polytope  $\Theta$ . More precisely, in this kind of LPV system, the state matrices range in a polytope of matrices defined as the convex hull of a finite number  $N$  of matrices. Each polytope vertex corresponds to a particular value of the scheduling variable  $\Psi_t$ . In other words:

$$\begin{pmatrix} A(\Psi_t) \\ B(\Psi_t) \end{pmatrix} \in \text{Co} \left\{ \begin{pmatrix} A_j \\ B_j \end{pmatrix}, j=1, \dots, N \right\} := \sum_{j=1}^N \alpha_t^j(\Psi_t) \begin{pmatrix} A_j \\ B_j \end{pmatrix} \quad (16)$$

with  $\alpha_t^j(\Psi_t) \geq 0$  and  $\sum_{j=1}^N \alpha_t^j(\Psi_t) = 1$ , where each  $j^{\text{th}}$  model is called a *vertex* system. Because of this property, this type of LPV systems is referred as polytopic.

A controller/observer can be designed for quasi-LPV system using these techniques by approximating the quasi-LPV system with a polytopic model. The simplest polytopic approximation relies on bounding each parameter by an interval. This approximation is known as *bounding box* approach. To obtain such an approximation, each of the element of the vector  $p_t$  is assumed to take values in an interval (e.g.  $\theta_h \in [\underline{\theta}_h, \bar{\theta}_h]$ ). Then, for each of the scheduling parameters in the vector  $\Psi_t$  their minimum and maximum values over the allowed values of the elements of  $p_t$  are calculated. For example, consider the parameter  $\Psi_t^1(p_t)$ . In this case, the extreme values  $\underline{\Psi}_t^1$  and  $\bar{\Psi}_t^1$  are given by:

$$\begin{aligned} \underline{\Psi}_t^1 &= -\left( k_a^2/R_a + B_{tr} + \max \{ k_{thp} \bar{\omega}_h, -k_{thm} \underline{\omega}_h \} \right) / J_{tr} \\ \bar{\Psi}_t^1 &= -\left( k_a^2/R_a + B_{tr} \right) / J_{tr} \end{aligned}$$

Taking into account all possible combinations of extreme values of the parameter vector elements, vertex systems in (16) are generated. The values of the non-linear model

TABLE I  
KNOWN AND UNKNOWN PARAMETERS

Param.	Value	Param.	Value	Param.	Value	Param.	Value
$r_{ts}$	0.1	$r_{ms}$	0.155	$J_{tr}$	?	$J_{mr}$	?
$l_t$	0.282	$l_m$	0.246	$B_{tr}$	?	$B_{mr}$	?
$l_b$	0.290	$l_{cb}$	0.276	$k_{thp/n}$	?	$k_{tvp/n}$	?
$m_b$	0.022	$m_{cb}$	0.068	$k_{fhp}$	?	$k_{fhn}$	?
$m_m$	0.014	$m_t$	0.015	$k_{jvp}$	?	$k_{jvn}$	?
$m_{mr}$	0.236	$m_{tr}$	0.221	$k_{chp}$	?	$k_{chn}$	?
$m_{ms}$	0.219	$m_{ts}$	0.119	$k_{cvp}$	?	$k_{cvn}$	?
$k_1$	6.5	$k_2$	8.5	$k_m$	?	$k_t$	?
$R_{ah/av}$	8	$L_{ah/av}$	0.86e-3	$k_{oh}$	?	$k_{ov}$	?
$k_g$	0.2	$k_{ah/av}$	0.0202				

parameters must be known in order to calculate the vertex systems for control design purposes. Some of these values are given by the manufacturer while others need to be estimated. This leads to the necessity of performing system identification.

There are several ways for implementing (16) depending on how  $\alpha_t^j(\Psi_t)$  functions are defined [14]. Here, the function  $\alpha_t^j(\Psi_t)$  is calculated via barycentric combination of vertices as suggested by [12].

### III. TWIN ROTOR MIMO SYSTEM IDENTIFICATION

In this section, the identification procedure to estimate the parameters of TRMS is presented (see Table I for the list of known and unknown parameters). At first, the unknown parameters of motor-propellers are identified. Then, those of the aerodynamical part are estimated. The spirit of the method is to compare, at each step, the data obtained from the real set-up with the data obtained by simulating part of the TRMS continuous-time non-linear model. This is included in an optimization problem so as to find the parameter values that give simulation results that better approximate the real system in a least squares fashion.

#### A. Tail and Main Propeller

The identification procedure is based on the knowledge of the non-linear model of the tail ((1) and (7)) and main propellers ((4) and (10)) and should identify some values for the unknown parameters in such a manner that the model behaviour resembles the real behaviour of the tail and main propellers. It is assumed to have at disposal  $N_\omega$  sets of data  $u_{h/v}^i(k), \omega_{h/v}^i(k)$  for the propellers where  $i = 1, \dots, N_\omega$  and  $k = 1, \dots, K_i$  where  $K_i$  is the number of samples of the  $i$ -th set of data. The identification procedure finds the minimum of the following objective function over the unknown parameters  $J_{tr/mr}, B_{tr/mr}, k_{th/vp}$  and  $k_{th/vn}$ :

$$J_\omega = \sum_{i=1}^{N_\omega} \sum_{k=1}^{K_i} \left( \omega_{h/v}^i(k) - \hat{\omega}_{h/v}^i(k) \right)^2 \quad (17)$$

where  $\hat{\omega}_{h/v}^i(k)$  is the simulation provided by Eqs. (1) and (4). Notice that, while all the sets of data can be used to identify  $J_{tr/mr}$  and  $B_{tr/mr}$ , a numerical value for  $k_{thp/vp}$  can be obtained only from those sets of data where the input voltage  $u_{h/v}$  is positive. Analogously, a numerical value for  $k_{thn/vn}$  can be obtained only from those sets of data where the input voltage  $u_{h/v}$  is negative.

## B. Tail Propeller to Horizontal Aeromechanics

The identification procedure is based on the knowledge of the non-linear model (2), (3), (8), (9), (12). In this step, the horizontal dynamics due to an input voltage acting on the tail propeller are identified (unknown parameters:  $k_{fhp}$ ,  $k_{fhn}$ ,  $k_{oh}$ ,  $k_{chp}$ ,  $k_{chn}$ ). When no input voltage acts on the main propeller, (2) and (3) simplify to:

$$\frac{d\Omega_h}{dt} = \frac{l_1 f_2(\omega_h) \cos \theta_v^0 - k_{oh} \Omega_h - f_3(\theta_h)}{D \cos^2 \theta_v^0 + E \sin^2 \theta_v^0 + F} \quad (18)$$

$$\frac{d\theta_h}{dt} = \Omega_h \quad (19)$$

Replacing (19) in (18) and using Laplace transform leads to:

$$\Theta_h(s) = \frac{K}{1 + 2\xi T_w s + T_w^2 s^2} \Psi_h(s) \quad (20)$$

where  $\Psi_h(s)$  is the Laplace transform of  $\omega_h^2(t)$  and:

$$K = \begin{cases} \frac{l_1 k_{fhp} \cos \theta_v^0}{k_{chp}} i f \omega_h \geq 0 & 2\xi T_w = \frac{k_{oh}}{k_{chp/n}} \\ -\frac{l_1 k_{fhn} \cos \theta_v^0}{k_{chn}} i f \omega_h < 0 & T_w^2 = \frac{D \cos^2 \theta_v^0 + E \sin^2 \theta_v^0 + F}{k_{chp/n}} \end{cases} \quad (21)$$

Hence, the knowledge of  $K$ ,  $\xi$  and  $T_w$  can be used for estimation of the unknown parameters:

$$\begin{aligned} k_{chp/n} &= \frac{K^{(p)}}{(T_w^{(p/n)})^2} k_{oh}^{(p/n)} & k_{fhp} &= \frac{K^{(p)} k_{chp}}{l_1 \cos \theta_v^0} \\ k_{oh}^{(p/n)} &= 2\xi^{(p/n)} T_w^{(p/n)} k_{chp/n} & k_{fhn} &= \frac{-K^{(n)} k_{chn}}{l_1 \cos \theta_v^0} \end{aligned} \quad (22)$$

Values for  $K^{(p)}$  and  $K^{(n)}$  can be found in a simple way through the knowledge of the steady-state values of  $\omega_h$  and  $\theta_h$ :

$$K^{(p/n)} = \theta_h^\infty / (\omega_h^\infty)^2 \quad (23)$$

Values for  $T_w^{(p)}$ ,  $T_w^{(n)}$ ,  $\xi^{(p)}$  and  $\xi^{(n)}$  can be estimated by means of some optimization method. It is assumed to have at disposal  $N_h$  sets of data  $\omega_h^i(k)$  and  $\theta_h^i(k)$  where  $i = 1, \dots, N_h$ ,  $k = 1, \dots, K_i$  and  $K_i$  is the number of samples of the  $i$ -th set of data. By applying the described procedure to each set of data, different values for the unknown parameters can be obtained. Such values can be used to define lower bounds and upper bounds for the values of the unknown parameters. Then, another identification stage can be performed. In this stage the minimum of the objective function over the unknown parameters ( $k_{fhp}$ ,  $k_{fhn}$ ,  $k_{oh}$ ,  $k_{chp}$ ,  $k_{chn}$ ):

$$J_h = \sum_{i=1}^{N_h} \sum_{k=1}^{K_i} \left( \theta_h^i(k) - \hat{\theta}_h^i(k) \right)^2 \quad (24)$$

should be found, where  $\hat{\theta}_h^i(k)$  is the solution of (18)-(19).  $\hat{\theta}_h$  can be calculated by considering that both  $\omega_h$  and  $\theta_v$  are data provided from the sensors.

## C. Main Propeller to Horizontal Aeromechanics

In this step, the horizontal dynamics due to an input voltage acting on the main propeller are identified (unknown parameters:  $k_m$ ,  $k_{cvp}$ ,  $k_{cvn}$ ). When no input voltage acts on the tail propeller, (2) and (3) simplify to:

$$\begin{aligned} \frac{d\Omega_h}{dt} &= \frac{k_m \omega_v \sin \theta_v \Omega_v (D \cos^2 \theta_v - E \sin^2 \theta_v - F - 2E \cos^2 \theta_v)}{(D \cos^2 \theta_v + E \sin^2 \theta_v + F)^2} \\ &+ \frac{-k_{oh} \Omega_h - f_3(\theta_h) + f_6(\theta_v)}{D \cos^2 \theta_v + E \sin^2 \theta_v + F} \\ &+ \frac{k_m \cos \theta_v \left( \frac{k_a k_2}{R_a} u_v - \left( B_{mr} + \frac{k_a^2}{R_a} \right) \omega_v - f_4(\omega_v) \right)}{J_{mr} (D \cos^2 \theta_v + E \sin^2 \theta_v + F)} \end{aligned} \quad (25)$$

$$\frac{d\theta_h}{dt} = \Omega_h \quad (26)$$

It is assumed to have at disposal  $M_h$  sets of data  $\omega_h^i(k)$ ,  $\theta_h^i(k)$  and  $\theta_v^i(k)$  where  $i = 1, \dots, M_h$ , and  $K_i$  is the number of samples of the  $i$ -th set of data. The identification procedure should identify values for  $k_m$ ,  $k_{cvp}$  and  $k_{cvn}$ , as all other parameter values are given by the manufacturer or have been identified previously. If the input voltage in the main propeller is a step signal, at steady-state:

$$\Omega_v^\infty = \Omega_h^\infty = \frac{k_a k_2}{R_a} u_v - \left( B_{mr} + \frac{k_a^2}{R_a} \right) \omega_v - f_4(\omega_v) = 0 \quad (27)$$

and considering (25) it reduces to:

$$\begin{cases} -k_{chp} \theta_h^\infty + k_{cvp} (\theta_v^\infty - \theta_v^0)^2 = 0 & i f \theta_v \geq \theta_v^0 \\ -k_{chp} \theta_h^\infty + k_{cvn} (\theta_v^\infty - \theta_v^0)^2 = 0 & i f \theta_v < \theta_v^0 \end{cases} \quad (28)$$

A first estimation of  $k_{cvp}$  and  $k_{cvn}$  is obtained from (28) as:

$$k_{cvp/n} = \frac{k_{chp} \theta_h^\infty}{(\theta_v^\infty - \theta_v^0)^2} \quad (29)$$

Later,  $k_m$ ,  $k_{cvp}$  and  $k_{cvn}$  can be refined by solving an optimization problem with the same objective function (24) that has been previously used, optimizing over the parameters  $k_m$ ,  $k_{cvp}$  and  $k_{cvn}$ .

## D. Main Propeller to Vertical Aeromechanics

In this case, the identification procedure should identify the values of  $k_{fvp}$ ,  $k_{fvn}$  and  $k_{ov}$ . Eq. (5) and (6), when no input voltage acts on the tail propeller, simplify to:

$$\begin{aligned} \frac{d\Omega_v}{dt} &= \frac{l_m f_5(\omega_v) + k_g \Omega_h f_5(\omega_v) \cos \theta_v - k_{ov} \Omega_v}{J_v} \\ &- \frac{0.5 \Omega_h^2 H \sin 2\theta_v + g((A-B) \cos \theta_v - C \sin \theta_v)}{J_v} \end{aligned} \quad (30)$$

$$\frac{d\theta_v}{dt} = \Omega_v \quad (31)$$

At steady-state, as  $\Omega_h^\infty = 0$  and  $\Omega_v^\infty = 0$ :

$$\frac{l_m f_5(\omega_v^\infty) + g((A-B) \cos \theta_v^\infty - C \sin \theta_v^\infty)}{J_v} = 0 \quad (32)$$

Thus, a preliminary estimation of  $k_{fvp}$  and  $k_{fvn}$  can be obtained as:

$$k_{fvp} = \frac{g((B-A) \cos \theta_v^\infty + C \sin \theta_v^\infty)}{l_m (\omega_v^\infty)^2} \quad (33)$$

TABLE II  
IDENTIFIED PARAMETERS VALUES

Par.	Value	Par.	Value	Par.	Value	Par.	Value
$B_{lr}$	0.0097	$B_{mr}$	0.0032	$k_{thp}$	0.0032	$k_{thn}$	4.8951e-4
$J_{lr}$	0.0101	$J_{mr}$	0.0562	$k_t$	0	$k_m$	0.0122
$k_{fvp}$	0.0177	$k_{fvn}$	0.0154	$k_{oh}$	0.0154	$k_{ov}$	0.0326
$k_{fhp}$	0.0187	$k_{fhn}$	0.0271	$k_{fvp}$	0.4311	$k_{fvn}$	0.2850
$k_{chp}$	0.0085	$k_{chn}$	0.0043	$k_{cvp}$	0.0207	$k_{cvn}$	0.0094

$$k_{fvn} = -\frac{g((B-A)\cos\theta_v^\infty + C\sin\theta_v^\infty)}{l_m(\omega_v^\infty)^2} \quad (34)$$

Later, the minimum over  $k_{fvp}$ ,  $k_{fvn}$  and  $k_{ov}$  of the objective function:

$$J_v = \sum_{i=1}^{N_i} \sum_{k=1}^{K_i} \left( \theta_v^i(k) - \hat{\theta}_v^i(k) \right)^2 \quad (35)$$

where  $\hat{\theta}_v^i(k)$  is the solution of (30)-(31), should be found.  $\hat{\theta}_v$  can be calculated by considering that both  $\omega_v$  and  $\Omega_h$  are data provided from the sensors.

#### E. Tail Propeller to Vertical Aeromechanics

It has been noticed experimentally that when the main propeller is off, the TRMS remains in its equilibrium vertical angle  $\theta_v^0$  for each value of  $u_h$ . This suggests that  $k_t = 0$  is a good approximation of the real value of this constant.

### IV. RESULTS

#### A. Non-linear Identification Results

The identification procedure has been applied to sets of data that correspond to experiments that lasts 60 s, with a sample period of 0.01 s. Each set is the response of the system to a step input voltage signal with a pseudo-random binary sequence overlapped from 30 s to 60 s. The minima of (17), (24) and (35) are found by means of *fmincon* MATLAB function of the Optimization Toolbox. This function attempts to find a constrained minimum of a scalar function of several variables (in this case, the unknown parameters). This is generally referred to as constrained non-linear optimization or non-linear programming. Even though such a function does not give guarantees of being achieved the global optimum, it has been noticed that performing the same optima search through the more robust *genetic algorithms* (GA) led to similar results as those obtained through *fmincon* but needing more computing time. The values returned by the *fmincon* function are listed in Table II.

#### B. Polytopic Bounding Box Results

Once the parameters of the non-linear model have been identified, a polytopic quasi-LPV model can be obtained by applying the procedure described in Section II-C. The motor inputs  $u_h$  and  $u_v$  and each of the state variables that influence the values of the elements of the state-space matrix (15) is assumed to take values in an interval, as resumed in Table III. In order to design a digital controller, a discrete-time polytopic model is required. Here, this has been obtained

TABLE III  
STATE VARIABLES LIMITS

Var.	Min.	Max.	Var.	Min.	Max.
$u_h, u_v$	-2.5 V	2.5 V	$\Omega_h$	-2 rad/s	2 rad/s
$\omega_h$	-3.5 V	2.5 V	$\omega_v$	-1.8 V	1.8 V
$\theta_h$	-3.4 rad	2.4 rad	$\theta_v$	0.7 rad	1.7 rad

TABLE IV  
SCHEDULING PARAMETERS LIMITS

$\Psi_k^j$	$\underline{\Psi}_k^j$	$\overline{\Psi}_k^j$	$\Psi_k^j$	$\underline{\Psi}_k^j$	$\overline{\Psi}_k^j$
$\Psi_k^1$	0.9840	0.9903	$\Psi_k^2$	2.59e-4	0.0048
$\Psi_k^3$	0.9895	0.9975	$\Psi_k^4$	-0.0058	-7.04e-4
$\Psi_k^5$	-0.0013	-1.15e-4	$\Psi_k^6$	-0.0075	0.0070
$\Psi_k^7$	-0.0045	0.0156	$\Psi_k^8$	0.9947	0.9994
$\Psi_k^9$	0	0	$\Psi_k^{10}$	-0.0092	0.0254
$\Psi_k^{11}$	0	0.0247	$\Psi_k^{12}$	-0.0412	-0.0240

using Euler approximation with sampling time  $T_s = 0.01s^1$ . Minimum and maximum values for each of the elements of the scheduling vector  $\Psi_k$  have been calculated, and such values are listed in Table IV.

### V. VALIDATION OF THE CALIBRATED TRMS MODEL

In order to validate the values obtained by means of identification, the model has been tested with various inputs. The simulation of the non-linear model has been compared to the data obtained from the real system. Two different validation scenarios have been performed. In these validation scenarios the input voltages for both the main and the tail propeller are sinusoidal with mean values different from zero, as resumed in Table V.

The comparisons between the simulation data and the real data are shown in Fig.2, Fig.3, Fig.4, Fig.5, Fig.6 and Fig.7.

The validation scenarios show that the model approximates the behaviour of both the propellers in a quite perfect manner. Nevertheless, the model and the real system are not so close when comparing the yaw and pitch angle responses. Although many experiments have been done with different sets of data and input signals, it has been proved hard to improve the results without modifying the non-linear model of the system, due to unmodelled frictions (e.g. the torque of the friction force presented in [1]) that are very difficult to characterize because of their high non-linearity and change in time.

However, the results prove to be satisfactory, as the model has to be used for control purposes and the control loop will compensate the imperfections in the model.

<sup>1</sup>The discrete-time versions of  $\psi_t$  and  $p_t$  are referred to as  $\psi_k$  and  $p_k$ .

TABLE V  
INPUT VOLTAGES FOR VALIDATION OF THE TRMS MODEL

Scenario	Input	Mean value	Sine amplitude	Sine frequency
1	$u_h$	0.7 V	0.3 V	0.1 Hz
1	$u_v$	0.7 V	0.3 V	0.05 Hz
2	$u_h$	0.6 V	0.3 V	0.1 Hz
2	$u_v$	0.6 V	0.1 V	0.05 Hz

## VI. CONCLUSIONS AND FUTURE WORK

This paper has presented the experimental identification of the parameters of the TRMS non-linear model using data collected from the real laboratory setup. From this non-linear model, a quasi-LPV model has also been obtained and, later, transformed into a polytopic one. The model parameters have been calibrated by means of nonlinear least-square identification approach. The results have been validated and the model has proved to show good performances in approximating the real behavior of the rotors. Results concerning the mechanical part were not so good, probably due to the non-linear and non-repetitive effect of frictions.

As a future work, the model obtained in this paper will be used for control purposes, so as to test some LPV techniques with a real set-up. Moreover, methods for deriving polytopic models that reduce conservativeness will be investigated (e.g. *bounding diamonds*, *convex hulls*). Finally, further investigation in the modelling of the TRMS will be done so as to include the non-linear time-varying effects due to frictions that have been neglected or approximated.

## REFERENCES

- [1] A. Rahideh and M. H. Shaheed, "Mathematical Dynamic Modelling of a Twin-Rotor Multiple Input-Multiple Output System," *IMEchE Journal of Systems and Control Engineering*, vol. 221, no. 1, pp. 89–101, 2007.
- [2] C. Gabriel, "Modelling, Simulation and Control of a Twin Rotor MIMO-System," *Project Thesis at Department of Systems Engineering and Control of Universidad Politecnica de Valencia*, 2008.
- [3] H. V. Christensen, "Modelling and Control of a Twin-Rotor MIMO System," *Report of Department of Control Engineering Institute of Electronic Systems of Aalborg University*, 2006.
- [4] F. Nejari, D. Rotondo, V. Puig, and M. Innocenti, "LPV Modelling and Control of a Twin Rotor MIMO System," in *19th IEEE Mediterranean Conference on Control and Automation*, 2011.
- [5] S. Ahmad, A. Chipperfield, and M. O. Tokhi, "Dynamic modelling and open-loop control of a twin rotor multi-input multi-output system," *Proceedings of the Institution of Mechanical Engineers, Part I: Journal of Systems and Control Engineering*, vol. 216, no. 6, pp. 477–496, 2002.
- [6] I. Z. M. Darus, F. M. Aldebrez, and M. O. Tokhi, "Parametric Modelling of a Twin Rotor System using Genetic Algorithms," in *First International Symposium on Control, Communications and Signal Processing*, 2004.
- [7] M. S. Alam and M. O. Tokhi, "Modelling of a twin rotor system: a particle swarm optimization approach," *Proceedings of the Institution of Mechanical Engineers, Part G: Journal of Aerospace Engineering*, vol. 221, no. 3, pp. 353–374, 2007.
- [8] S. F. Toha, M. O. Tokhi, and Z. Hussain, "ANFIS Modelling of a Twin Rotor System," in *UKACC Control Conference*, 2008.
- [9] S. F. Toha and M. O. Tokhi, "Parametric modelling application to a twin rotor system using recursive least squares, genetic, and swarm optimization techniques," *Proceedings of the Institution of Mechanical Engineers, Part G: Journal of Aerospace Engineering*, vol. 224, no. 9, pp. 961–977, 2010.
- [10] A. Kwiatkowski, M. T. Boll, and H. Werner, "Automated Generation and Assessment of Affine LPV Models," *Proceedings of the 45th IEEE Conference on Decision and Control, San Diego, CA, USA*, pp. 6690–6695, 2006.
- [11] L. Ljung, *System Identification: Theory for the User*. Prentice Hall Information and System Sciences Series, 1987.
- [12] P. Apkarian, P. Gahinet, and G. Becker, "Self-scheduled  $H_\infty$  Control of Linear Parameter-Varying Systems: A Design Example," *Automatica*, vol. 31, no. 9, pp. 1251 – 1261, 1995.
- [13] M. Chilali and P. Gahinet, " $H_\infty$  Design with Pole Placement Constraints: An LMI Approach," *IEEE Transactions on Automatic Control*, vol. 41, no. 3, pp. 358–367, 1996.
- [14] R. Murray-Smith and T. A. Johansen, *Multiple Model Approaches to Modelling and Control*. Taylor and Francis, 1997.

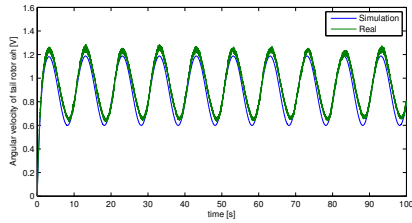


Fig. 2. Validation scenario 1: Angular velocity of tail rotor  $\omega_h$ .

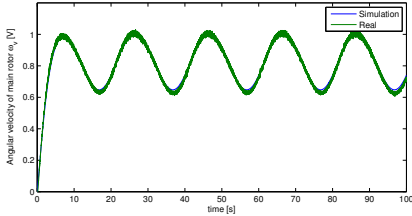


Fig. 3. Validation scenario 1: Angular velocity of main rotor  $\omega_v$ .

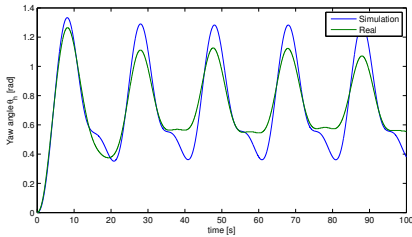


Fig. 4. Validation scenario 1: Yaw angle of the TRMS  $\theta_h$ .

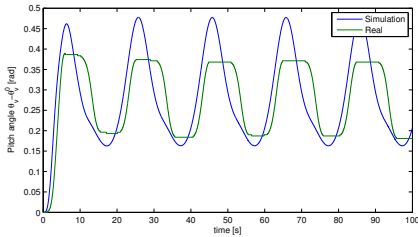


Fig. 5. Validation scenario 1: Pitch angle of the TRMS  $\theta_v - \theta_v^0$ .

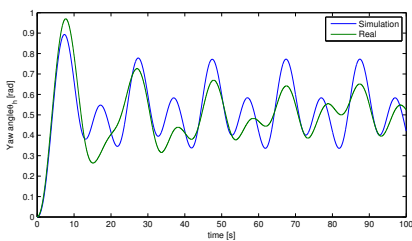


Fig. 6. Validation scenario 2: Yaw angle of the TRMS  $\theta_h$ .

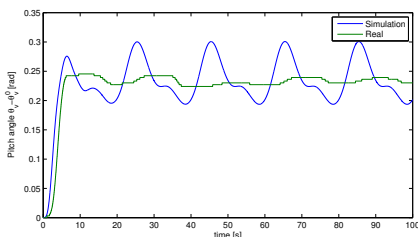


Fig. 7. Validation scenario 2: Pitch angle of the TRMS  $\theta_v - \theta_v^0$ .